

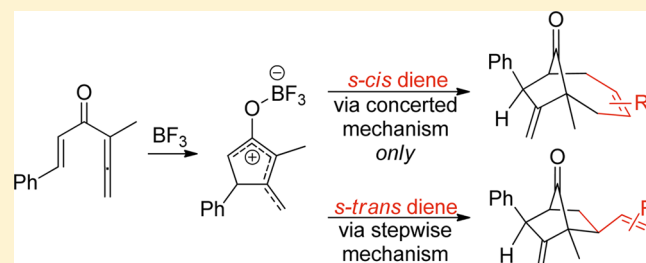
Computational Examination of (4 + 3) versus (3 + 2) Cycloaddition in the Interception of Nazarov Reactions of Allenyl Vinyl Ketones by Dienes

Zhe Li, Russell J. Boyd,* and D. Jean Burnell*

Department of Chemistry, Dalhousie University, P.O. Box 15000, Halifax, Nova Scotia B3H 4R2, Canada

S Supporting Information

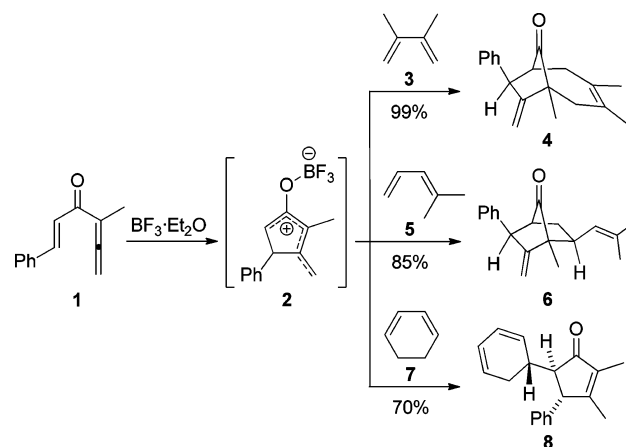
ABSTRACT: A computational examination of the tandem Nazarov/cycloaddition process involving an allenyl vinyl ketone with a diene has been carried out using the ω B97X-D/6-311++G(d,p)// ω B97X-D/6-31+G(d,p) method with solvation modeled by SMD-PCM. The barrier for the initial Lewis acid mediated Nazarov reaction, which provided the intermediate cyclic oxyallyl cation, was higher than that for any subsequent cycloaddition. The barrier for the first step of a subsequent stepwise reaction did not vary much with the diene, and the lowest barrier was with the diene in its *s-trans* conformation. Stepwise formation of a (4 + 3) cycloaddition product was not energetically feasible, but (3 + 2) cycloaddition products could have been produced through low energy pathways. The barrier for a concerted (4 + 3) cycloaddition did depend upon the diene, which was always in an *s-cis* geometry. The barriers for the compact and the extended geometries for the transition states of (4 + 3) cycloadditions were not much different.



INTRODUCTION

Allenyl vinyl ketones (AVKs) are especially reactive substrates for Nazarov reactions.¹ Tius has thoroughly explored the Nazarov reactions of ether-substituted AVKs,² but alkyl-substituted AVKs have received less attention. The Nazarov reactions of alkyl-substituted AVKs were first reported by Hashmi,³ and we showed that alkyl-substituted AVKs are well suited for “interrupted” Nazarov reactions.^{4,5} Of special note was the tandem process in which the cyclic delocalized cation that was the intermediate of the Nazarov reaction underwent cycloaddition with an acyclic 1,3-diene or an electron-rich alkene. These dienes could react by (4 + 3) or (3 + 2) cyclization,⁶ or both.^{7–10} As the products of (4 + 3) cycloaddition, which have seven-membered rings, are the more synthetically attractive,^{11,12} efforts have been made to identify the structural and electronic factors that promote (4 + 3) versus (3 + 2) cycloadditions involving oxyallyl cations generated by the Nazarov reactions of AVKs. The (4 + 3) versus (3 + 2) selectivity was dependent on the substitution on both the diene^{7–9} and the AVK.^{9,10} Less steric hindrance led to more (4 + 3) cycloaddition. For instance, diene 3 intercepted the cation 2, which was generated by the BF_3 -mediated Nazarov reaction of AVK 1, providing the (4 + 3) cycloaddition product 4 exclusively (Scheme 1). However, cation 2 cyclized with diene 5 only by (3 + 2) cycloaddition to give 6.⁷ Increasing the electron density of the diene also enhanced the (4 + 3) mode of cyclization.⁹ Cyclic dienes, such as furan and 1,3-cyclohexadiene 7, did not undergo cycloaddition with cation 2. Their products had only one new carbon–carbon bond between the AVK and diene moieties, such as in 8.⁷

Scheme 1. Interrupted Nazarov Reactions of AVK 1 in the Presence of Dienes 3, 5, and 7



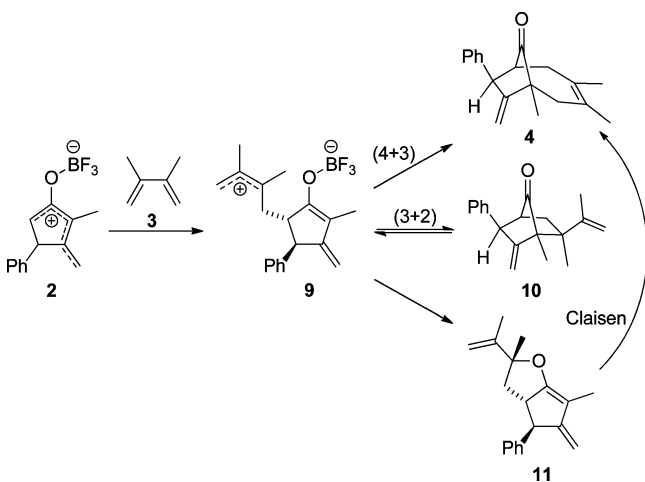
The mechanisms of cycloadditions onto cationic intermediates such as 2 are not well understood. It is accepted that the (3 + 2) cycloadditions take place by a stepwise mechanism because a concerted pathway would require an antarafacial transition state geometry. However, the (4 + 3) cycloadditions could be either stepwise or suprafacial-concerted. Evidence for a stepwise mechanism in the case of (4 + 3) cycloadditions of oxyallyl cation 2 is that the products of (4 + 3) cycloaddition

Received: October 15, 2015

Published: November 23, 2015

are not infrequently accompanied by (3 + 2) cycloaddition products and compounds with a single new carbon–carbon bond.¹¹ The implication is that an initial carbon–carbon bond forms, and then the allylic cation intermediate **9** could cyclize to the (4 + 3) product **4** or the (3 + 2) product **10** (Scheme 2),

Scheme 2. Hypothetical Stepwise Formation of the (4 + 3) Product **4 from the Oxyallyl Cation **2** with Diene **3****



or **9** might simply deprotonate to yield a compound with a single new carbon–carbon bond. Some (3 + 2) products have been rearranged to thermodynamically favored (4 + 3) products in the presence of the Lewis acid, but the rate of such rearrangement seems to be too slow to account for the proportion of the (4 + 3) products in the product mixtures

from the tandem Nazarov/cycloaddition reactions.^{7–9} Computational studies by Cramer and Barrows¹³ supported a stepwise mechanism for (4 + 3) cycloadditions involving butadiene and cyclic dienes.¹³ Two additional computational studies concluded that (4 + 3) cycloadditions involving furan are stepwise.^{14,15} Calculations also indicated that an intermediate such as **9** could cyclize onto the oxygen, giving an alternative (3 + 2) product **11**, which in turn could undergo Claisen rearrangement to give the (4 + 3) product **4**.¹³ Experimental evidence for a similar (3 + 2) cycloaddition/Claisen rearrangement process leading to a seven-membered ring had been reported two decades before the computational study.¹⁶ In the particular instance of the formation of **4**, the Claisen rearrangement would be feasible only for the diastereomer **11** shown in Scheme 2.

(4 + 3) Cycloadditions involving **2** and dienes may be considered to be $[4\pi + 2\pi]$ cycloadditions, just like classical Diels–Alder reactions, which are concerted. However, the reactions of allyl cations with dienes, which Gassman¹⁷ termed ionic Diels–Alder reactions, were deemed “so asynchronous as to be stepwise” based on experimental results.¹⁸ A stepwise mechanism for the ionic Diels–Alder reaction has been supported by a computational study,¹⁹ but more recent experiments have indicated that minor variations in the substrates can tip the reaction pathway toward a mechanism that was more clearly described as concerted.¹⁹

We have suggested that (4 + 3) cycloadditions involving **2** and acyclic dienes are concerted.^{7–9} A (4 + 3) cycloaddition like the one that produced **4** in 5 min at -78°C , whether it is stepwise or concerted, must take place with the diene in its *s-cis* conformation. Dienes for which the *s-cis* conformations are highly disfavored give (3 + 2) products, which can form when

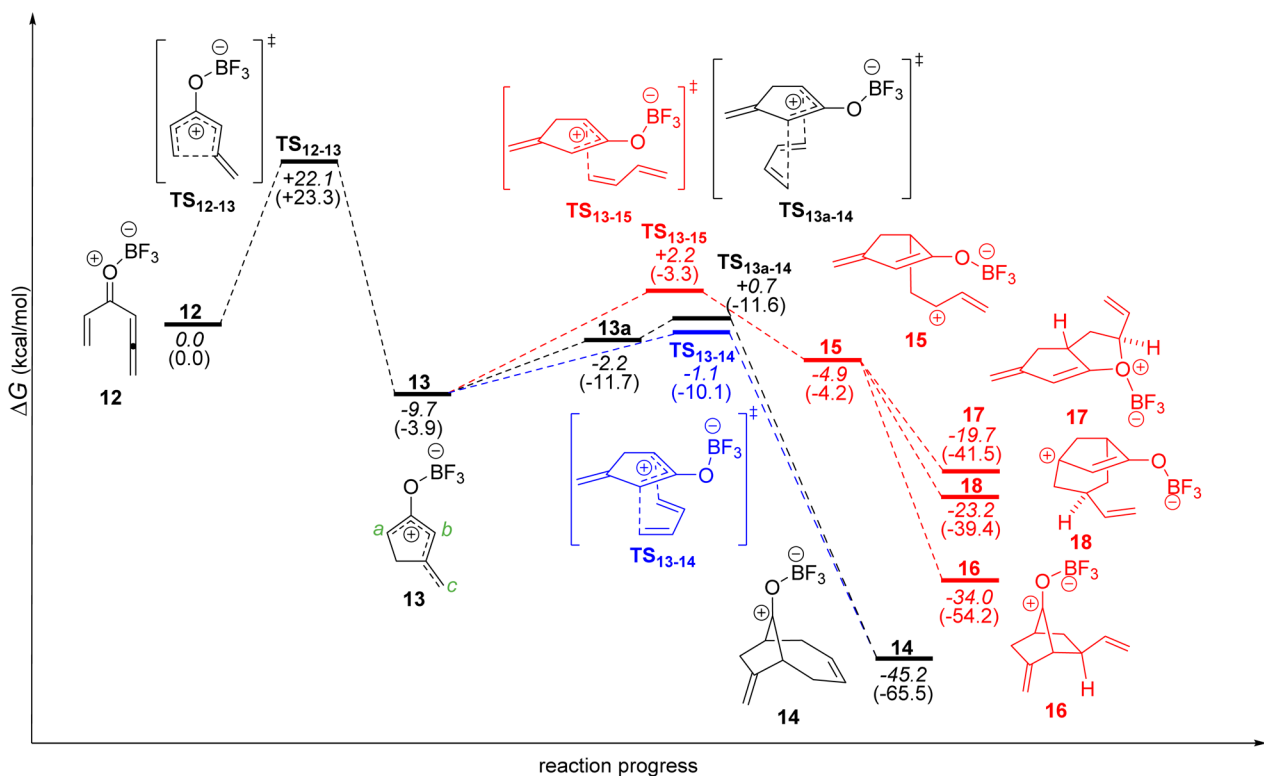


Figure 1. Gibbs energy profile for the tandem BF_3 -mediated Nazarov/cycloaddition reactions of AVK **12** with 1,3-butadiene. Gibbs energies in kcal/mol ($\omega\text{B97X-D}/6\text{-311++G(d,p)}/\omega\text{B97X-D}/6\text{-31+G(d,p)}$ using SMD-PCM: CH_2Cl_2) are in italics with the enthalpies in gas phase in parentheses.

dienes react in their *s-trans* conformations.^{7,8} Thus, there are alternative pathways available for oxyallyl cations to react with dienes in the more accessible *s-trans* conformations, but, nevertheless, (4 + 3) cycloaddition products predominate in many instances. The *s-cis* conformer of a diene must react more quickly with **2** than an *s-trans* conformer in order to produce mainly a (4 + 3) product in either a stepwise or a concerted mechanism. There is computational support for some concerted (4 + 3) cycloadditions. Whereas the intramolecular cycloaddition of furan was stepwise, Fernández and co-workers¹⁴ found that the cycloaddition of the corresponding acyclic diene was concerted and fairly synchronous. Similarly, Cramer and Harmata²⁰ found an intramolecular (4 + 3) cycloaddition of a cyclic oxyallyl cation with an acyclic diene to be concerted. Thus, the mechanism for the (4 + 3) cycloaddition to the cation derived by the Nazarov reaction of an AVK is unclear. The motivation for the present contribution was to explore both the (4 + 3) and the (3 + 2) cycloaddition mechanisms through a computational study that compared a number of possible reaction pathways involving dienes and a cyclic oxyallyl cation derived from the Nazarov reaction of an AVK.

COMPUTATIONAL METHODS

All quantum mechanical calculations were performed with the *Gaussian 09* software package.²² For computational studies of (4 + 3) reactions of allyl cations with various dienes, Cramer and co-workers^{13,21} had employed MP2/6-31(d)//RHF/6-31(d) and MP2/6-31(d). They deemed the second-order perturbation method to be more reliable than the B3LYP density functional, which they also used. Nevertheless, much more recently Fernández and co-workers¹⁴ used the B3LYP/def2-SVP level for calculations, and West and co-workers¹⁵ optimized their geometries with B3LYP/6-311+G(d,p).

We chose the dispersion-corrected ω B97X-D density functional²³ at the 6-31+G(d,p) level of theory for geometry optimizations in the gas phase. This density functional had served well in a related study.⁸ Minima and first-order saddle points were characterized by their number of imaginary frequencies following normal-mode vibrational analysis, i.e., 0 and 1, respectively. The intrinsic reaction coordinate (IRC) method²⁴ was used when the geometry of the transition state was very different from the starting material and the product, and the vibrational mode of the negative frequency did not show a clear connection. Single point energies were calculated at ω B97X-D/6-311+G(d,p). All geometries and thermodynamic data were obtained from calculations done in the gas phase at 298.15 K and 1.0 atm. The tandem Nazarov/cycloaddition processes that this computational study was seeking to model involved charged species. Even though the solvent used experimentally was dry CH₂Cl₂,^{7,8} an organic solvent of modest polarity, the solvation Gibbs energies were calculated using the SMD continuum solvation method²⁵ with CH₂Cl₂ as the solvent at the ω B97X-D/6-31+G(d,p) level.

RESULTS AND DISCUSSION

Model System: AVK 12 with 1,3-Butadiene. In order to explore the mechanistic possibilities of this reaction with less computational cost, a model reaction of the simplest AVK **12** with 1,3-butadiene was investigated first. Experimentally, in the presence of BF₃·Et₂O, AVK **12** reacted more rapidly by a Diels–Alder reaction with diene **3** than it did by the tandem Nazarov/cycloaddition process.¹⁰ The BF₃-mediated Nazarov reaction of **12** took place via transition state TS_{12–13} with a barrier of +22.1 kcal/mol to produce the oxyallyl cation **13** (Figure 1). The enthalpic change on going to transition state TS_{12–13} was about the same. The geometry of TS_{12–13} was very

similar to the computed transition states in a recent computational study of Nazarov reactions of AVKs.²⁶

The cycloaddition of **13** and 1,3-butadiene could be either concerted or stepwise. Along a concerted pathway, a reaction complex **13a** of **13** with the diene was found that led to the transition state TS_{13a–14} with an extended (exo) geometry. The counterpart complex leading to the transition state TS_{13–14} with compact (endo) geometry was not located. The Gibbs energy of **13a** was 7.5 kcal/mol higher than that of **13**, but the enthalpy was lower than that of **13** by 7.8 kcal/mol. The enthalpy of transition state TS_{13a–14} was only 0.1 kcal/mol higher than that of **13a**, indicating that the potential energy surface was flat around the transition state, and therefore it was not surprising that the geometries of **13a** and TS_{13a–14} were similar, also. The lengths of the two incipient carbon–carbon bonds in TS_{13a–14} were only slightly shorter than the corresponding distances in **13a**. The Gibbs energy barrier of the extended transition state TS_{13a–14} was 10.4 kcal/mol while the Gibbs energy of the compact transition state TS_{13–14} was 8.6 kcal/mol. In terms of enthalpic change the transition states were much lower in energy than the oxyallyl cation **13** plus the *s-cis* diene, which reflected the considerable stabilization attendant upon the formation of new carbon bonds. The incipient carbon–carbon bonds in TS_{13–14} were much longer than the incipient bonds in TS_{13a–14} (Figure 2), and the incipient bonds that were much

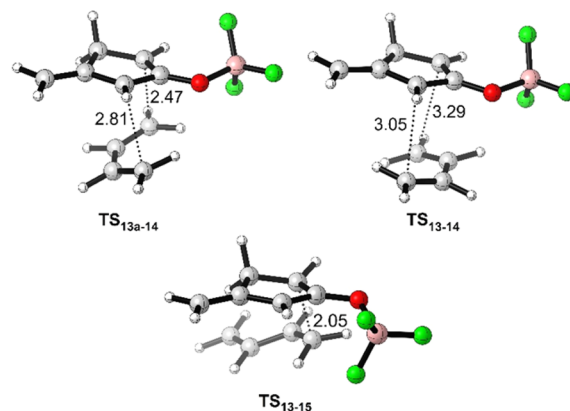


Figure 2. Geometries of three transition states for the tandem BF₃-mediated Nazarov/cycloaddition reactions of AVK **12** with 1,3-butadiene. Distances are in ångströms.

longer than in transition states with other dienes (see below). IRC analysis of TS_{13–14} pointed to a potential energy surface about the transition state that was very flat.²⁷ The geometry optimization of the product from TS_{13–14} converged to the same (4 + 3) product **14** as the product from TS_{13a–14}. The change in Gibbs energy for the cycloaddition was –35.5 kcal/mol, and the change in enthalpy was –61.6 kcal/mol.

A stepwise attack by 1,3-butadiene might take place at any one of three carbons of the oxyallyl cation **13** (*a*, *b*, and *c*), but only attack at the most electrophilic site (*a*)¹⁰ was considered here. The attack by the diene in its *s-trans* conformation had a lower barrier than the attack by the diene in its *s-cis* conformation of the diene (Figure S1 in the Supporting Information). This was consistent with the HOMO energy of the *s-trans* diene being higher than that of the *s-cis* diene (–8.45 eV versus –8.68 eV). Thus, TS_{13–15} had the lowest barrier, +11.9 kcal/mol, of the stepwise transition states. However, this barrier was still higher than that for either concerted transition

state, and so a stepwise pathway would not be followed to a significant extent. The difference in the calculated barriers was larger in the gas phase than in CH_2Cl_2 solution because of greater stabilization of TS_{13-15} than of either concerted transition state. The incipient carbon–carbon bond in TS_{13-14} was 0.5 Å shorter than the corresponding incipient bond in either concerted transition state (Figure 2), which indicated that the stepwise transition state was later than the concerted ones. TS_{13-15} led to the allylic cation 15 for which the Gibbs energy was higher than that for the oxyallyl cation 13 with 1,3-butadiene, although the enthalpy was almost the same. Isomerization of an allylic cation such as 15 into the geometry necessary for further cyclization to a (4 + 3) product would not be feasible because the barrier for the carbon–carbon bond rotation has been estimated to be over 30 kcal/mol.²⁸ The (3 + 2) product 16 that could arise from 15 was much higher in Gibbs energy and enthalpy than the (4 + 3) product 14. The procedure to reveal the subsequent steps of the stepwise reaction pathway were as follows. A relaxed potential energy scan was made by rotating the diene moiety along the newly formed carbon–carbon bond of 15 to 180° in both directions at a step size of 5°. At each point of the scan, the geometry was optimized at $\omega\text{B97X-D}/6-31+\text{G}(\text{d})$ with the fixed dihedral angle of the diene moiety. This led to the identification of the cyclized structures 17 and 18, of which the former represented the type of (3 + 2) product predicted by Cramer and Barrows.¹³ However, the relative stereochemistry of 17 precluded Claisen rearrangement to 14. Compound 18, which the calculations indicated was lower in Gibbs energy and enthalpy than 17 in spite of having a nonplanar allylic cation, arose from cyclization of 15 from the end of the exocyclic double bond of 15 onto the allyl cation.

In order for the stepwise Claisen rearrangement route¹³ to the (4 + 3) product 14 to be possible, the oxygen-included (3 + 2) product would have to be 19, the epimer of 17. An extensive search for transition states leading from the oxyallyl cation 13 and 1,3-butadiene to 19 was carried out, but the only transition state located was for a concerted cyclization TS_{13-19} with the diene in its *s-trans* conformation (Figure 3). The barrier was +14.3 kcal/mol, which was higher than the barriers of both of the concerted (4 + 3) and the stepwise transition states shown in Figure 1. The product derived from TS_{13-19} was 19, which was lower in Gibbs energy than 17. Then, 19 had to undergo rotation about a carbon–carbon bond to 19a before the Claisen rearrangement, via transition state TS_{19a-14} , to the (4 + 3) product 14 could take place. The barrier for the Claisen rearrangement was +12.6 kcal/mol, which was lower than that for the (3 + 2) step.

AVK 1 with 2,3-Dimethyl-1,3-butadiene (3). Attention was directed next toward tandem reactions for which experimental results were available. The barrier for the Nazarov reaction of AVK 1 was 14.0 kcal/mol, which was 8.1 kcal/mol lower than that of AVK 12, and the formation of oxyallyl cation 2 was more exothermic than the formation of 13 (Figure 4). This was consistent with the slower Nazarov reactions observed experimentally with AVK 12 relative to AVK 1.¹⁰ However, the barrier for the formation of 2 was still higher than subsequent cycloaddition steps by both the stepwise and the concerted mechanisms. The barriers of the concerted (4 + 3) transition states, which proceeded from the reaction complexes 2a and 2b, were +10.1 and +11.3 kcal/mol for the extended and compact transition states TS_{2a-4a} and TS_{2b-4b} , respectively. Thus, in this instance, the extended transition state had the

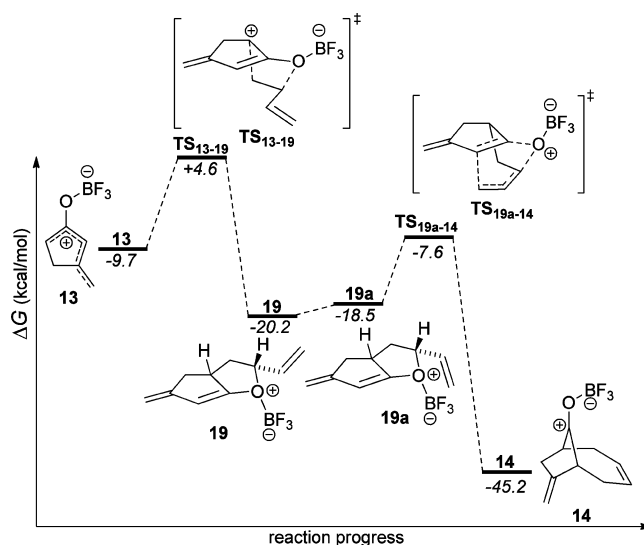


Figure 3. Gibbs energy profile in kcal/mol ($\omega\text{B97X-D}/6-31++\text{G}(\text{d,p})//\omega\text{B97X-D}/6-31+\text{G}(\text{d,p})$ using SMD-PCM: CH_2Cl_2) for the oxygen-included (3 + 2) cyclization of oxyallyl cation 13 with 1,3-butadiene and then Claisen rearrangement to 14. Enthalpies are in parentheses.

lower barrier. (The immediate products of these concerted reactions were different conformations of 4: 4a and 4b.) As for the simpler system, there was considerable enthalpic stabilization from the cycloaddition that was evident even at the transition states. The incipient bond lengths indicated that the degree of synchronicity was approximately the same as in the case of the (4 + 3) cycloadditions of the model system. The incipient carbon–carbon bonds at position a of the oxyallyl cation 2 were shorter than those at position b, and the distances of the corresponding incipient carbon–carbon bonds were very similar in TS_{2a-4a} and TS_{2b-4b} (Figure 5). The geometry of the extended transition state TS_{2a-4a} was remarkably similar in terms of barrier and geometry to the corresponding transition state with 1,3-butadiene, TS_{13a-14} .

The HOMO energy for diene 3 in its *s-trans* conformation was -8.38 eV, and for the *s-cis* conformer the HOMO energy was -8.46 eV. In the stepwise mechanism, the transition states with *s-cis* conformations of 3 were not favored. (See Figure S2 in the Supporting Information.) The stepwise transition state with the lowest energy was TS_{2-19} with a barrier of +12.4 kcal/mol, and the incipient carbon–carbon bond length was 2.16 Å. This transition state led to the allyl cation 19, the epimer of allyl cation 9 in Scheme 2 (Figure 4). This barrier was higher than that for either concerted pathway. Thus, the (4 + 3) product 4 was predicted for the tandem Nazarov/cycloaddition, which was in agreement with the experimental result.⁷ Efforts to locate a transition state for the cyclization of 19 to the (3 + 2) product 20 were unsuccessful. (Neither 20 nor its epimer was detected experimentally.⁷) Instead, the attempts to locate the elusive transition state were repeatedly diverted to TS_{9-21} , with a barrier of +6.3 kcal/mol, that led to compound 21, which was much lower in Gibbs energy than 20. The incipient carbon–carbon bond length in TS_{19-21} was 2.70 Å. It was interesting that 21 had the same ring system as products of Lewis acid mediated rearrangement of some (3 + 2) products. For instance, the BF_3 -mediated Nazarov reaction of AVK 1 with diene 22 at -78 °C had quickly given epimeric (3 + 2) cycloaddition products 23, but in the presence of BF_3 some 23

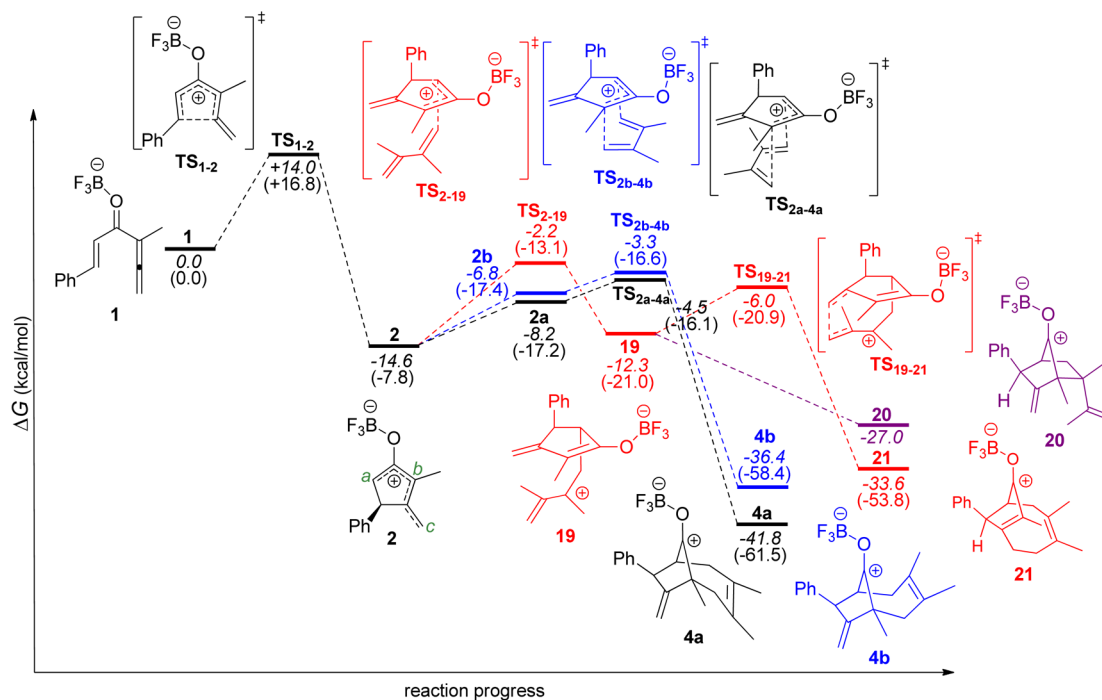


Figure 4. Gibbs energy profile for the tandem BF_3 -mediated Nazarov/cycloaddition reactions of AVK **1** with diene **3**. Gibbs energies in kcal/mol ($\omega\text{B97X-D}/6\text{-311++G(d,p)}/\omega\text{B97X-D}/6\text{-31+G(d,p)}$ using SMD-PCM: CH_2Cl_2) are in italics; the enthalpies are in parentheses.

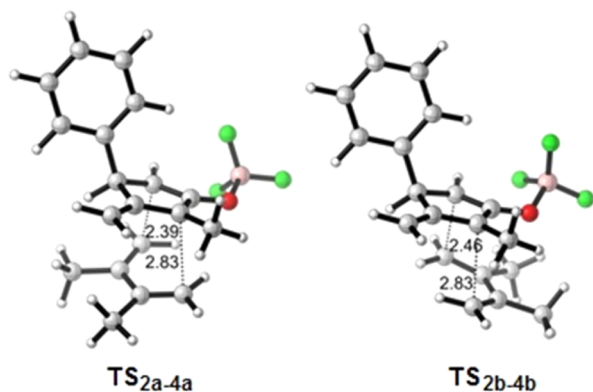
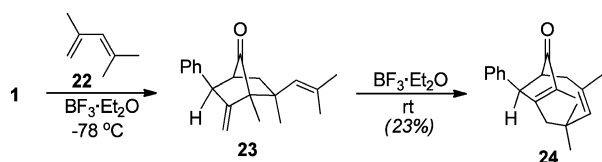


Figure 5. Geometries of the transition states of the (4 + 3) cycloadditions of oxyallyl cation **2** with diene **3**. Distances are in ångströms.

rearranged at rt to the more stable compound **24** (Scheme 3).^{7,8}

In a recent study of torquoselectivity in the Nazarov reactions of AVKs, differences between the computed and experimentally determined torquoselectivities led to the hypothesis that the tandem (4 + 3) cycloaddition reaction was exaggerating the apparent torquoselectivities of the Nazarov reactions.²⁶ The torquoselectivity study employed AVKs with a

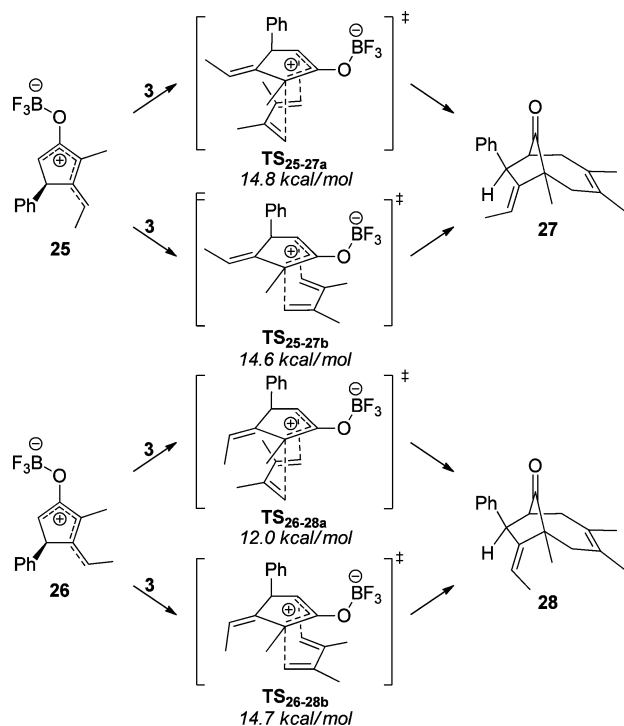
Scheme 3. Formation of the (3 + 2) Cycloaddition Product **23** and Its Rearrangement to **24**



substituent on the terminus of the allene. The alternative products from the Nazarov reaction were oxyallyl cations that differed in the geometry of their exocyclic double bond. The computational work with diene **3** was extended to the (4 + 3) cycloadditions with oxyallyl cations **25** and **26**, which represent the “inward-rotation” and “outward-rotation” alternatives, respectively, of a torquoselective Nazarov reaction (Scheme 4). The extended (TS_{25-27a} and TS_{26-28a}) and the compact (TS_{25-27b} and TS_{26-28b}) transition states were located. The geometries of the extended transition states were very similar to that of TS_{2a-4a} in Figure 5, and likewise the compact transition states were very similar to TS_{2b-4b} . A methyl group on the exocyclic double bond of the oxyallyl cation had a detrimental effect on the (4 + 3) cycloaddition with diene **3** because all four barriers in Scheme 4 were higher than those with the unmethylated oxyallyl cation, i.e., TS_{2a-4a} and TS_{2b-4b} . Nevertheless, one of the transition states shown in Scheme 4, TS_{26-28a} , had a significantly lower barrier than the other three. The “outward-rotation” isomer **26** should react more readily, via TS_{26-28a} , than the “inward-rotation” isomer **25** with diene **3**, and so the proportion of a mixture of the isomers should be enhanced in favor of the “outward-rotation” product by subsequent cycloaddition. Experimentally, the “outward-rotation” products, e.g. **28**, were preponderant over the “inward-turn” products, e.g. **27**.²⁶

AVK 1 with 4-Methyl-1,3-pentadiene (5). The formation of the oxyallyl cation **2** was the same as in Figure 4. Both the concerted and stepwise mechanisms of the cycloaddition of **2** with diene **5** were examined. In contrast with 1,3-butadiene and with diene **3**, the barriers of the concerted transition states TS_{2c-29} and TS_{2d-29} that led from the reaction complexes **2c** and **2d** were approximately 3 kcal/mol higher than the barrier for the stepwise transition state TS_{2-30} involving diene **5** in its *s-trans* conformation (Figure 6). (The HOMO energy for *t-trans* **5** was -7.95 eV. The HOMO energy for *s-cis* **5** was -8.16 eV.)

Scheme 4. (4 + 3) Cycloaddition of Diene 3 to Isomeric Oxyallyl Cations 25 and 26 with the Activation Energy for Each Concerted Reaction Pathway Computed Using ω B97X-D/6-311++G(d,p)// ω B97X-D/6-31+G(d,p)



As in the case of the other systems, all interactions of the oxyallyl cation 2 with diene 5 reduced the enthalpy.

The concerted transition states were more asynchronous than in the previous systems. The new carbon–carbon bond at position *a* in 2 was shorter than in the previous examples, and the new carbon–carbon bond at position *b* was about 3.3 Å (Figure 7), which was much longer. This was very likely the

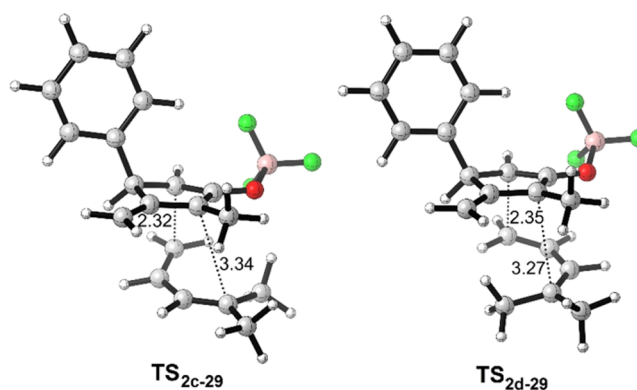


Figure 7. Geometries of the transition states TS_{2c-29} and TS_{2d-29} for the (4 + 3) cycloadditions of oxyallyl cation 2 with diene 5. Distances are in ångströms.

result of the steric repulsion caused by the two methyl substituents on the terminus of diene 5. In light of this hindrance it was not surprising that the barriers for both concerted cycloaddition pathways were higher than the concerted pathways with diene 3. In the stepwise pathway, the barrier for transition state TS₂₋₃₀ was 11.4 kcal/mol, and the incipient bond length was 2.30 Å. The allyl cation 30 was slightly lower in Gibbs energy relative to 2, in contrast with similar intermediates in the model reaction (Figure 1) and in the reaction of 2 with diene 3 (Figure 4). Ring closure of 30 gave the (3 + 2) product 6 via TS₃₀₋₆ with a barrier of only +1.7 kcal/mol.²⁹ A relatively long incipient carbon–carbon bond of 3.10 Å of TS₃₀₋₆ was consistent with an early transition state. Thus, with diene 5 the stepwise (3 + 2) cycloaddition pathway was kinetically favored over the concerted (4 + 3) cycloaddition pathway, even though the (4 + 3) product was more stable.

AVK 1 with 1,3-Cyclohexadiene (7). 1,3-Cyclohexadiene (7), with its diene moiety fixed in an *s-cis* arrangement and with

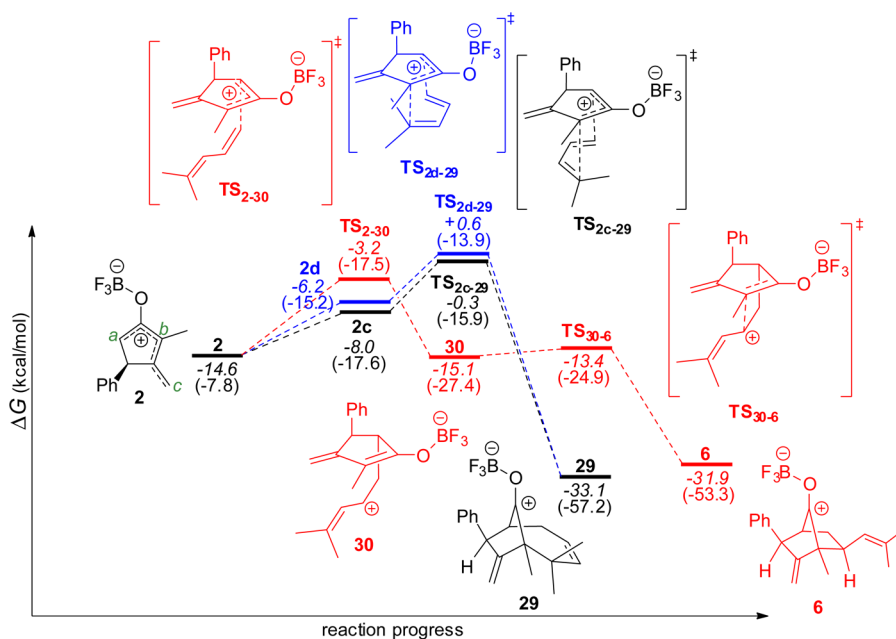


Figure 6. Gibbs energy profile for the tandem BF₃-mediated Nazarov/cycloaddition reactions of oxyallyl cation 2 with diene 5. Gibbs energies in kcal/mol (ω B97X-D/6-311++G(d,p)// ω B97X-D/6-31+G(d,p) using SMD-PCM: CH₂Cl₂) are in italics; the enthalpies are in parentheses.

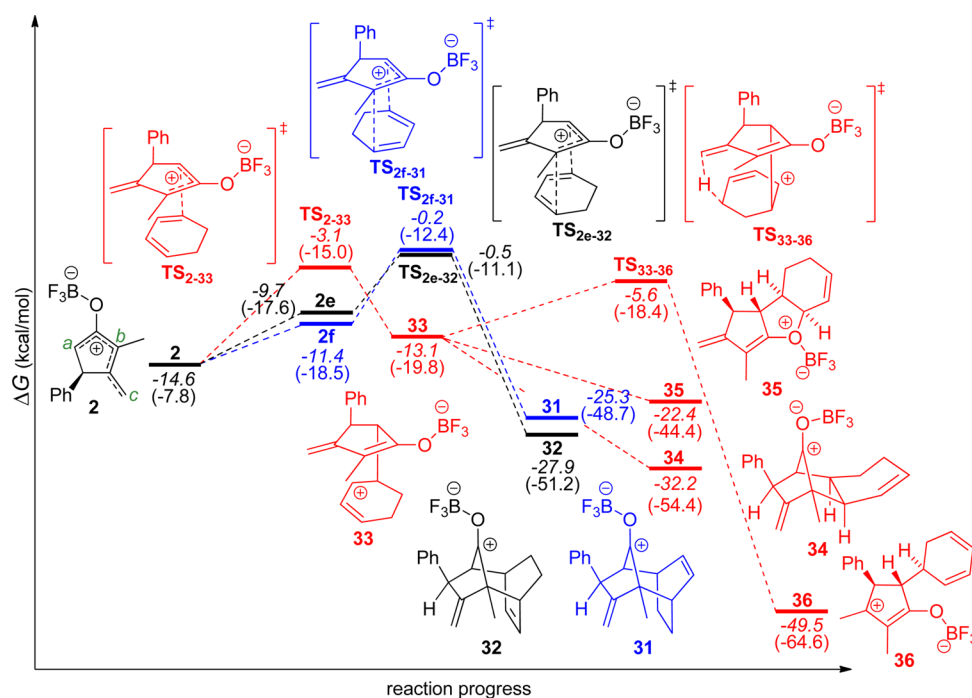


Figure 8. Gibbs energy profile for the tandem BF_3 -mediated Nazarov/cycloaddition reactions of oxallyl cation **2** with diene **7**. Gibbs energies in kcal/mol ($\omega\text{B97X-D}/6\text{-311++G(d,p)}/\omega\text{B97X-D}/6\text{-31+G(d,p)}$) using SMD-PCM: CH_2Cl_2) are in italics; the enthalpies are in parentheses.

a HOMO energy of -7.89 eV, was found experimentally to react with the oxallyl cation **2** to form a single new carbon–carbon bond to give **8** (Scheme 1).⁷ This reaction can be viewed as the initial carbon–carbon bond-forming step at position *a* of **2**, which had been seen in the previous three systems to be the result of reaction of the diene in its *s-trans* conformation. In their DFT computational research, West and co-workers were unable to locate any concerted (4 + 3) transition state for the reaction of the oxallyl cation derived from a divinyl ketone and another cyclic diene, furan.¹⁵

Concerted transition states for both the compact ($\text{TS}_{2\text{f-31}}$) and extended ($\text{TS}_{2\text{e-32}}$) (4 + 3) cycloadditions were located for **2** with 1,3-cyclohexadiene (**7**) (Figure 8). (In the process, reactant complexes **2e** and **2f** were identified.) The barriers for $\text{TS}_{2\text{f-31}}$ and $\text{TS}_{2\text{e-32}}$ were 14 kcal/mol above the energy of **2**, and these two barriers were essentially the same. Thus, if any (4 + 3) product could be detected, the expectation would be for a 1:1 mixture of the isomeric products **31** and **32**. These transition states were highly nonsynchronous (Figure 9). This was especially the case for $\text{TS}_{2\text{f-31}}$, where the incipient bond at position *b* of the oxallyl cation was 4.25 Å, and the reactants were twisted relative to each other such that the terminus of the diene could barely be considered to be subtending position *b* of **2**. In fact, the shorter incipient bond in $\text{TS}_{2\text{f-31}}$ was similar in length to the length of the incipient bond in TS_{2-33} for the stepwise reaction, but the IRC for $\text{TS}_{2\text{f-31}}$ showed a smooth reduction of energy to the product **31**. The barrier of the initial carbon–carbon bond forming reaction for TS_{2-33} was +11.5 kcal/mol, which was similar to what it had been for TS_{13-15} , TS_{2-19} , and TS_{2-30} , for 1,3-butadiene and for dienes **3** and **5**. This was 2.6 kcal/mol lower in Gibbs energy than for a concerted transition state. TS_{2-33} had the same orientation as the concerted, extended transition state $\text{TS}_{2\text{e-32}}$, and TS_{2-33} led to the allyl cation **33**, but the Gibbs energy of **33** was higher than that for **2**. (The stepwise transition state that resembled the compact transition state $\text{TS}_{2\text{e-32}}$ is not shown in Figure 8

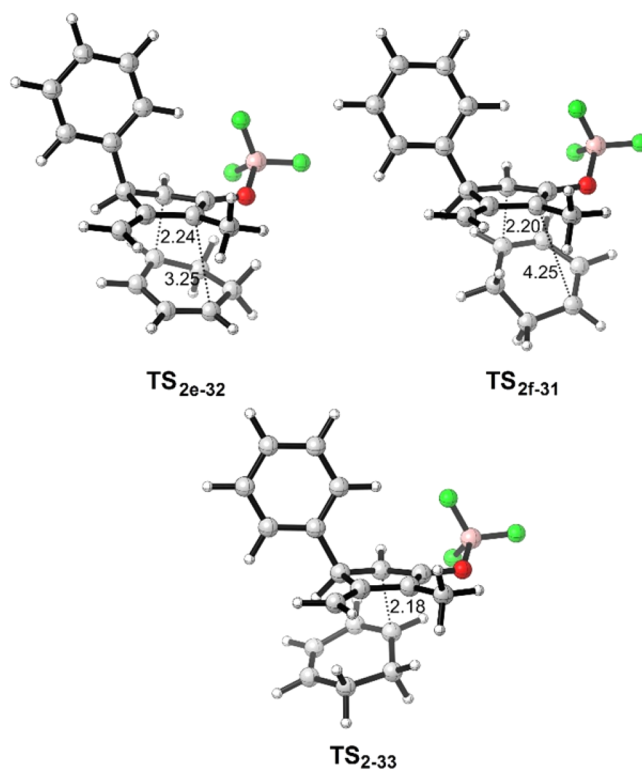


Figure 9. Geometries of the transition states $\text{TS}_{2\text{e-32}}$, $\text{TS}_{2\text{f-31}}$, and TS_{2-33} for the cycloadditions of oxallyl cation **2** with diene **7**. Distances are in Ångströms.

because its barrier was 2.6 kcal/mol higher than that of TS_{2-33} .) A search for transition states for the cyclization of **33** was unsuccessful. The expected (3 + 2) product **34** was much lower in Gibbs energy than **33**. The oxygen-included (3 + 2) product **35** had a higher Gibbs energy than **34**, but the Gibbs energy of

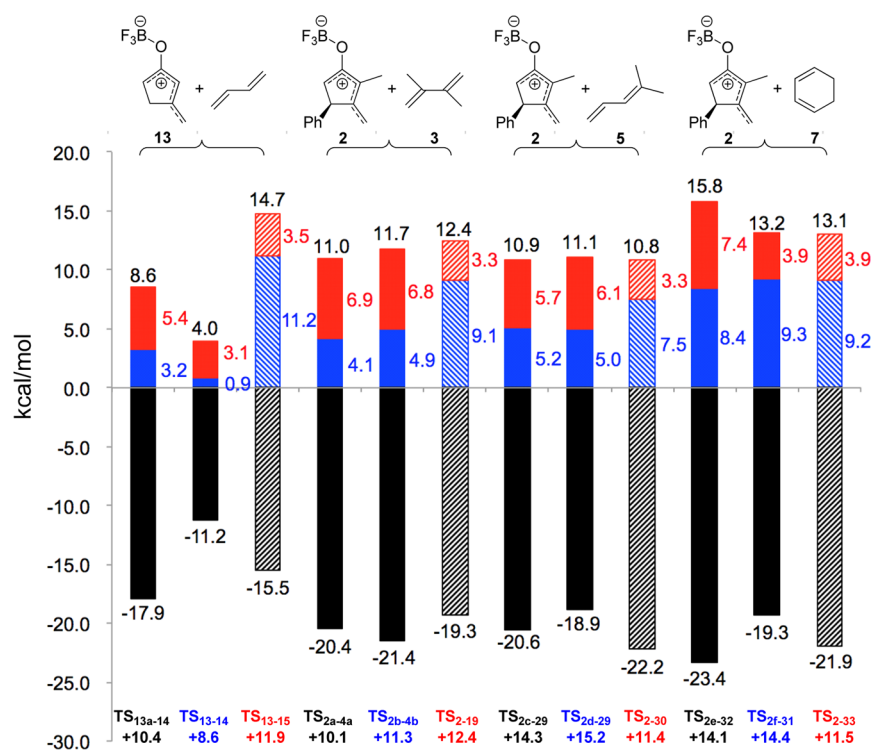


Figure 10. Deformation and interaction energies (kcal/mol) of transition states in (4 + 3) concerted cycloaddition and stepwise carbon-carbon bond formation pathways. Deformation energies of the dienes are red, deformation energies of the oxyallyl cations are blue, and the interaction energies are black. The energies of the concerted transition states are in solid colors, and those of stepwise transition states are in diagonal lines. The Gibbs energy barriers (kcal/mol) of the transition states are given at the bottom of the figure.

35 was still much lower than that of 33. A transition state connecting 33 to 35 could not be found either, but a relaxed potential energy scan along the forming carbon-oxygen bond showed a smooth decrease in energy (Figure S5 in the Supporting Information). This indicated that the formation of 35 from 33 had a low barrier. An intramolecular prototropy reaction of 33 produced 36 that would yield 8 after workup. The transition state was located as TS₃₃₋₃₆ with barriers of +9.0 kcal/mol relative to 2. If 35 was formed, it might undergo reversible ring opening to 33 and then produce 36 via TS₃₃₋₃₆. That 34 was not observed experimentally implied that 8, which was the actual product of this reaction,⁷ arose by prototropy in 33.

Selectivity. The activation energies (ΔG^\ddagger) for the four stepwise transition states (TS₇₋₁₀, TS₂₋₁₇, TS₂₋₂₄, and TS₂₋₂₉) were within 1 kcal/mol of each other, whereas the activation energies for the concerted reactions ranged from 8.6 to 15.2 kcal/mol. The concerted reactions had lower barriers via extended geometries except for the reaction of 13 with 1,3-butadiene.

In an effort to identify what controls extended versus compact (4 + 3) cycloadditions and (4 + 3) versus (3 + 2) cycloaddition selectivities, an examination of the deformation energies for the reactants and the interaction energies at the various transition states was undertaken. Applications of such analyses by ourselves³⁰ and by others³¹ have been successful in clarifying the origins of selectivity in Diels-Alder and other cycloaddition reactions. The difference in energy (ΔE) between the diene in its lowest-energy conformation and the isolated diene in its transition state geometry is the “diene deformation energy.” The corresponding energy for the oxyallyl cation is the “oxyallyl cation deformation energy.” Subtraction of the two

deformation energies from the activation energy (ΔE^\ddagger) gives the “interaction energy.” The deformation and interaction energies of the transition states in the concerted (4 + 3) cycloaddition and stepwise pathways studied above are provided in Figure 10. In the concerted reactions, the diene and the oxyallyl cation deformation energies tend to be similar whereas the oxyallyl cation deformation energy was consistently larger than the diene deformation energy for the stepwise transition states.

Overall, however, Figure 10 reveals no clear correlation between any component of the transition state energies and selectivity. One of the partners in these cycloadditions, the oxyallyl cation, is very reactive relative to the addends in previously examined reactions. This means that the reaction between the oxyallyl cation and a diene, whether the reaction is concerted or stepwise, is associated with a large reduction in the enthalpy, which translates into large, negative interaction energies at the transition states. Thus, the interaction energies, which could include both the strong attractive as well as some repulsive interactions, overwhelm the contributions of deformation. This is in contrast with analyses of Diels-Alder reactions³⁰ in which the interaction energies were smaller and fairly constant, but the deformation of the diene correlated strongly with the selectivity.

CONCLUSIONS

The mechanism of the tandem Nazarov/cycloaddition reaction of allenyl vinyl ketones has been examined in detail computationally. The Nazarov reaction has a significantly higher barrier than the subsequent cycloaddition. The interaction of the immediate product of the Nazarov reaction, a cyclic oxyallyl cation, leads to a considerable reduction in the

enthalpy. Stepwise reactions of the oxyallyl cation with dienes have lower barriers with *s-trans* dienes than with *s-cis* dienes, whereas (4 + 3) cycloadditions of dienes with the oxyallyl cation are concerted and therefore involve *s-cis* dienes. The simplest system of oxyallyl cation **13** with 1,3-butadiene underwent (4 + 3) cycloaddition preferentially via a compact transition state geometry, whereas the (4 + 3) cycloadditions of oxyallyl cation **2** with dienes **3**, **5**, and **7** all favored extended transition state geometries. When the transition states for the concerted (4 + 3) cycloadditions were very nonsynchronous, as described by the differences in the lengths of the incipient carbon-carbon bonds, then a stepwise reaction of the oxyallyl cation had a lower barrier. After the initial step in the stepwise process had taken place, there were very low barriers to different modes of cyclization. The resulting products included the (3 + 2) cycloaddition product and the oxygen-included (3 + 2) cycloaddition product first proposed by Cramer and Barrows, but the latter product would have had the wrong relative stereochemistry for sigmatropic rearrangement into the (4 + 3) cycloaddition product. The (4 + 3) versus (3 + 2) cycloaddition selectivity could not be correlated with the energy to deform either the diene or the oxyallyl cation (or both) due to a dominance of strongly attractive interactions between the diene and the oxyallyl cation at the transition state.

■ ASSOCIATED CONTENT

Supporting Information

The Supporting Information is available free of charge on the ACS Publications website at DOI: 10.1021/acs.joc.5b02397.

Full Gibbs energy diagrams for the stepwise reactions of AVK **12** with 1,3-butadiene and of AVK **1** with dienes **3**, **5**, and **7**; relaxed potential energy scan along the C–O bond of **35**; Cartesian coordinates, energies, and frequencies for computed structures (PDF)

■ AUTHOR INFORMATION

Corresponding Authors

*E-mail: russell.boyd@dal.ca.

*E-mail: jean.burnell@dal.ca.

Notes

The authors declare no competing financial interest.

■ ACKNOWLEDGMENTS

We are grateful to the Natural Sciences and Engineering Research Council of Canada for financial support of this research (RGPIN/9-2013 and RGPIN/1480-2012). High performance computational facilities were provided by the Atlantic Computational Excellence Network (ACEnet). ACEnet is funded by the Canada Foundation for Innovation (CFI), the Atlantic Canada Opportunities Agency (ACOA), and the provinces of Newfoundland and Labrador, Nova Scotia, and New Brunswick.

■ REFERENCES

- (1) Reviews: (a) Nakanishi, W.; West, F. G. *Curr. Opin. Drug Discovery Dev.* **2009**, *12*, 732–751. (b) Vaidya, T.; Eisenberg, R.; Frontier, A. J. *ChemCatChem* **2011**, *3*, 1531–1548. (c) Shimada, N.; Stewart, C.; Tius, M. A. *Tetrahedron* **2011**, *67*, 5851–5870.
- (2) Review: Tius, M. A. *Chem. Soc. Rev.* **2014**, *43*, 2979–3002.
- (3) Hashmi, A. S. K.; Bats, J. W.; Choi, J.-H.; Schwarz, L. *Tetrahedron Lett.* **1998**, *39*, 7491–7494.

(4) Review of “interrupted” Nazarov reactions: Grant, T. N.; Rieder, C. J.; West, F. G. *Chem. Commun.* **2009**, 5676–5688.

(5) (a) Marx, V. M.; Burnell, D. J. *Org. Lett.* **2009**, *11*, 1229–1231. (b) Marx, V. M.; Cameron, T. S.; Burnell, D. J. *Tetrahedron Lett.* **2009**, *50*, 7213–7216. (c) Marx, V. M.; LeFort, F. M.; Burnell, D. J. *Adv. Synth. Catal.* **2011**, *353*, 64–68. (d) Boudreau, J.; Courtemanche, M.-A.; Marx, V. M.; Burnell, D. J.; Fontaine, F.-G. *Chem. Commun.* **2012**, *48*, 11250–11252.

(6) Herein (4 + 3) and (3 + 2) refer to the number of carbons implicated in the cycloaddition processes, not the number of π -electrons.

(7) Marx, V. M.; Burnell, D. J. *J. Am. Chem. Soc.* **2010**, *132*, 1685–1689.

(8) Morgan, T. D. R.; LeFort, F. M.; Li, Z.; Marx, V. M.; Boyd, R. J.; Burnell, D. J. *Eur. J. Org. Chem.* **2015**, *2015*, 2952–2959.

(9) LeFort, F. M.; Mishra, V.; Dexter, G. D.; Morgan, T. D. R.; Burnell, D. J. *J. Org. Chem.* **2015**, *80*, 5877–5886.

(10) Marx, V. M.; Stoddard, R. L.; Heverly-Coulson, G. S.; Burnell, D. J. *Chem. - Eur. J.* **2011**, *17*, 8098–8104.

(11) Harmata, M. *Chem. Commun.* **2010**, *46*, 8886–8903 and references therein.

(12) For reviews emphasizing some synthetic aspects of (4 + 3) cycloadditions: (a) Hartung, I. V.; Hoffmann, H. M. R. *Angew. Chem., Int. Ed.* **2004**, *43*, 1934–1947. (b) Battiste, M. E.; Pelphrey, P. M.; Wright, D. L. *Chem. - Eur. J.* **2006**, *12*, 3438–3447. (c) Harmata, M. *Adv. Synth. Catal.* **2006**, *348*, 2297–2306. (d) Harmata, M. *Chem. Commun.* **2010**, *46*, 8904–8922. (e) Lohse, A. G.; Hsung, R. P. *Chem. - Eur. J.* **2011**, *17*, 3812–3822.

(13) (a) Cramer, C. J.; Barrows, S. E. *J. Org. Chem.* **1998**, *63*, 5523–5532. (b) Cramer, C. J.; Barrows, S. E. *J. Phys. Org. Chem.* **2000**, *13*, 176–186.

(14) Fernández, I.; Cossío, F. P.; de Cozár, A.; Lledós, A.; Mascareñas, J. L. *Chem. - Eur. J.* **2010**, *16*, 12147–12157.

(15) Wu, Y.-K.; Dunbar, C. R.; McDonald, R.; Ferguson, M. J.; West, F. G. *J. Am. Chem. Soc.* **2014**, *136*, 14903–14911.

(16) Chidgey, R.; Hoffmann, H. M. R. *Tetrahedron Lett.* **1978**, *19*, 1001–1004.

(17) (a) Gassman, P. G.; Gorman, D. B. *J. Am. Chem. Soc.* **1990**, *112*, 8623–8624. (b) Gorman, D. B.; Gassman, P. G. *J. Org. Chem.* **1995**, *60*, 977–985 and references therein.

(18) Gassman, P. G.; Gorman, D. B. *J. Am. Chem. Soc.* **1990**, *112*, 8624–8626.

(19) de Pascual-Teresa, B.; Houk, K. N. *Tetrahedron Lett.* **1996**, *37*, 1759–1763.

(20) Ko, Y.-J.; Shim, S.-B.; Shin, J.-H. *Tetrahedron Lett.* **2007**, *48*, 863–867.

(21) Cramer, C. J.; Harmata, M.; Rashatasakhon, P. *J. Org. Chem.* **2001**, *66*, 5641–5644.

(22) Frisch, M. J.; Trucks, G. W.; Schlegel, H. B.; Scuseria, G. E.; Robb, M. A.; Cheeseman, J. R.; Scalmani, G.; Barone, V.; Mennucci, B.; Petersson, G. A.; Nakatsuji, H.; Caricato, M.; Li, X.; Hratchian, H. P.; Izmaylov, A. F.; Bloino, J.; Zheng, G.; Sonnenberg, J. L.; Hada, M.; Ehara, M.; Toyota, K.; Fukuda, R.; Hasegawa, J.; Ishida, M.; Nakajima, T.; Honda, Y.; Kitao, O.; Nakai, H.; Vreven, T.; Montgomery Jr., J. A.; Peralta, J. E.; Ogliaro, F.; Bearpark, M.; Heyd, J. J.; Brothers, E.; Kudin, K. N.; Staroverov, V. N.; Keith, T.; Kobayashi, R.; Normand, J.; Raghavachari, K.; Rendell, A.; Burant, J. C.; Iyengar, S. S.; Tomasi, J.; Cossi, M.; Rega, N.; Millam, J. M.; Klene, M.; Knox, J. E.; Cross, J. B.; Bakken, V.; Adamo, C.; Jaramillo, J.; Gomperts, R.; Stratmann, R. E.; Yazyev, O.; Austin, A. J.; Cammi, R.; Pomelli, C.; Ochterski, J. W.; Martin, R. L.; Morokuma, K.; Zakrzewski, V. G.; Voth, G. A.; Salvador, P.; Dannenberg, J. J.; Dapprich, S.; Daniels, A. D.; Farkas, O.; Foresman, J. B.; Ortiz, J. V.; Cioslowski, J.; Fox, D. J. *Gaussian 09*, Revision D.01; Gaussian, Inc.: Wallingford, CT, 2013.

(23) (a) Chai, J.-D.; Head-Gordon, M. *J. Chem. Phys.* **2008**, *128*, 084106–15. (b) Chai, J.-D.; Head-Gordon, M. *Phys. Chem. Chem. Phys.* **2008**, *10*, 6615–6620.

(24) (a) Fukui, K. *Acc. Chem. Res.* **1981**, *14*, 363–375. (b) Gonzalez, C.; Schlegel, H. B. *J. Chem. Phys.* **1989**, *90*, 2154–2161. (c) Collins, M.

A. *Theor. Chem. Acc.* **2002**, *108*, 313–324. (d) Hratchian, H. P.; Schlegel, H. B. *J. Chem. Phys.* **2004**, *120*, 9918–9924. (e) Hratchian, H. P.; Schlegel, H. B. *J. Chem. Theory Comput.* **2005**, *1*, 61–69.

(25) Marenich, A. V.; Cramer, C. J.; Truhlar, D. G. *J. Phys. Chem. B* **2009**, *113*, 6378–6396.

(26) Morgan, T. D. R.; LeBlanc, L. M.; Ardagh, G. H.; Boyd, R. J.; Burnell, D. J. *J. Org. Chem.* **2015**, *80*, 1042–1051.

(27) The geometry of TS_{13-14} at B3LYP/6-31+G(d,p) was very similar. The incipient bonds were 3.30 and 3.18 Å. B3LYP functional: (a) Becke, A. D. *Phys. Rev. A: At., Mol., Opt. Phys.* **1988**, *38*, 3098–3100. (b) Lee, C.; Yang, W.; Parr, R. G. *Phys. Rev. B: Condens. Matter Mater. Phys.* **1988**, *37*, 785–789. (c) Becke, A. D. *J. Chem. Phys.* **1993**, *98*, 1372–1377. (d) Becke, A. D. *J. Chem. Phys.* **1993**, *98*, 5648–5852.

(28) (a) Mayr, H.; Förner, W.; Schleyer, P. v. R. *J. Am. Chem. Soc.* **1979**, *101*, 6032–6040. (b) Dorigo, A. E.; Li, Y.; Houk, K. N. *J. Am. Chem. Soc.* **1989**, *111*, 6942–6948.

(29) This barrier was calculated in the gas phase because the energy of TS_{30-6} was calculated to be 1.4 kcal/mol lower than **30** when solvation Gibbs energies were compared. Small differences between the potential energy surfaces in gas phase and in solution should be expected.

(30) (a) Poirier, R. A.; Pye, C. C.; Xidos, J. D.; Burnell, D. J. *J. Org. Chem.* **1995**, *60*, 2328–2329. (b) Pye, C. C.; Xidos, J. D.; Poirier, R. A.; Burnell, D. J. *J. Phys. Chem. A* **1997**, *101*, 3371–3376. (c) Xidos, J. D.; Poirier, R. A.; Pye, C. C.; Burnell, D. J. *J. Org. Chem.* **1998**, *63*, 105–112. (d) Liu, P.-Y.; Wu, Y.-J.; Pye, C. C.; Thornton, P. D.; Poirier, R. A.; Burnell, D. J. *Eur. J. Org. Chem.* **2012**, *2012*, 1186–1194.

(31) (a) Ess, D. H.; Houk, K. N. *J. Am. Chem. Soc.* **2007**, *129*, 10646–10647. (b) Lam, Y.; Cheong, P. H.-Y.; Blasco Mata, J. M.; Stanway, S. J.; Gouverneur, V.; Houk, K. N. *J. Am. Chem. Soc.* **2009**, *131*, 1947–1957. (c) Hayden, A. E.; Houk, K. N. *J. Am. Chem. Soc.* **2009**, *131*, 4084–4089. (d) Gordon, C. G.; Mackey, J. L.; Jewett, J. C.; Sletten, E. M.; Houk, K. N.; Bertozzi, C. R. *J. Am. Chem. Soc.* **2012**, *134*, 9199–9208. (e) Hong, X.; Liang, Y.; Griffith, A. K.; Lambert, T. H.; Houk, K. N. *Chem. Sci.* **2014**, *5*, 471–475.